Effect of Molecular Crowding on Conformation and Interactions of Single-Chain Nanoparticles

Julian Oberdisse, Marina Gonzalez-Burgos, Ander Mendia, Arantxa Arbe, Angel J. Moreno, Jose A. Pomposo, Aurel Radulescu, Juan Colmenero

Effect of Molecular Crowding on Conformation and Interactions of Single-Chain Nanoparticles

Julian Oberdisse[a,b]*, Marina González-Burgos[c], Ander Mendia[c], Arantxa Arbe[c]*, Angel J. Moreno[b,c], José A. Pomposo[c,d,e], Aurel Radulescu[f] and Juan Colmenero[b,c,d]

[a]*Laboratoire Charles Coulomb (L2C), University of Montpellier, CNRS, 34095 Montpellier, France*

[b]*Donostia International Physics Center (DIPC), Paseo Manuel de Lardizabal 4, 20018 San Sebastián, Spain*

[c]*Materials Physics Center (MPC), Centro de Física de Materiales (CFM) (CSIC-UPV/EHU), Paseo Manuel de Lardizabal 5, 20018 San Sebastián, Spain*

[d]*Departamento de Física de Materiales, Universidad del País Vasco (UPV/EHU), Apartado 1072, 20080 San Sebastian, Spain*

[e]*IKERBASQUE – Basque Foundation for Science, María Díaz de Haro 3, 48013 Bilbao, Spain*

[f]*Forschungszentrum Jülich GmbH, Jülich Centre for Neutron Science JCNS at Heinz Maier-Leibnitz Zentrum MLZ, 85748 Garching, Germany.*

* Authors for correspondence: julian.oberdisse@umontpellier.fr; a.arbe@ehu.eus

Abstract

The conformation of single-chain nanoparticles (SCNPs) in presence of linear polystyrene crowding molecules has been studied by small-angle neutron scattering under contrast-matching of the crowders. A model describing the scattering of aggregating polydisperse SCNPs has been developed, resulting in the determination of the potentially squeezed size of the individual SCNPs within aggregates, their local chain statistics, and the average aggregation number, as a function of crowding. Two different crowders – of low and high molecular weight, respectively – are shown to have a different effect: while long chains tend to impede their aggregation above their overlap concentration, short ones are found to mediate depletion interactions leading to aggregation. Self-imposed crowding within the aggregates has a similar impact on chain conformation independently of the crowding of the surrounding medium. Our results are compared to recent simulations and shall contribute to the microscopic understanding of the phase behavior of soft intrinsically disordered nano-objects, and in particular the effect of crowding on biomacromolecules.

Keywords: single-chain nanoparticles, macromolecular conformation, aggregation modeling, small-angle neutron scattering, macromolecular crowding, intrinsically disordered nano-objects

Introduction

Single-chain nanoparticles (SCNPs) are soft disordered nano-objects synthesized by intra-molecular bonding of linear polymer chains with a finite fraction of reactive groups [1-3]. The folding/collapse process leading to SCNP formation has attracted significant interest as a simplified model of protein folding [4,5], or as protein mimics in general [6,7]. Moreover, studies combining synthesis, scattering experiments and simulations have revealed striking analogies between SCNPs and intrinsically disordered proteins (IDPs) [8,9]. As shown by small-angle scattering techniques and coarse-grained molecular dynamics (MD) simulations[10], the statistical properties of SCNPs in dilute solution follow a close to ideal behavior due to internal crosslinking. The MD-simulations reveal that SCNPs are characterized by a highly complex network of internal rings ('loops') interconnected into clusters. This internal compartmentalization, together with their softness and ultra-small size, are features that could be of utmost interest for their applications in nano-technology: Sensing capabilities, controlled drug delivery and catalytic applications of SCNPs have been recently demonstrated [11-20].

Though not recognized until very recently, IDPs play also a relevant role in a wide variety of biological processes [21] and are also involved in different diseases [22]. As shown by Moreno et al [8], in dilute solutions SCNPs and IDPs exhibit similar scaling laws and the presence of intramolecular compact and weakly deformable domains connected by very flexible segments; also, dynamical analogies like the similar influence of the internal friction have been reported [9,23]. In most of the studies the properties of biomolecules are characterized in vitro under high dilution [24], while biologically relevant conditions involve complex environments including macromolecules of different chemical composition and sizes, and where crowding is an unavoidable –and determining – ingredient.

The spatial conformation of IDPs and its evolution depending on the cellular environment are topical issues [25-27]. Understanding them demands for relatively simple models of IDPs allowing

the separation of molecular crowding from specific interactions usually present in proteins. Therefore, SCNPs, free of strong specific interactions characteristic for proteins, can be taken as simple model systems to separately investigate the effects of crowding of purely steric origin (excluded volume effects) on the structural and dynamical properties of IDPs in cellular environments. In addition, the investigation of crowding effects on SCNPs is of high intrinsic interest due to, *e.g.*, their potential biomedical applications [28], including their use in cellular environments [29]. MD-simulations[8] revealed that SCNPs in concentrated solutions and in bulk collapse into 'crumpled globular' structures [30,31], instead of adopting the random-walk conformation [32] characteristic of linear chains.

The experimental determination of the structure and dynamics of a particular macromolecule in a crowded environment requires combining scattering techniques with labelling methods ('hiding' the crowders in the sea of solvent). Small-angle scattering is a powerful method used to study aggregation [33,34] and dispersion [35] phenomena in bulk systems. Applying neutron scattering on contrast-matched systems allows obtaining microscopic information in many-component systems, in particular in presence of crowders [36]. The effects of crowding on the conformation of poly(methyl methacrylate) (PMMA)-based SCNPs in deuterated solvent were recently explored [37]. As crowders, similar (deuterated) SCNPs were considered. However, increasing the concentration of SCNPs led to unavoidable macromolecular aggregation above a concentration of $c^*_{NP}/3$ (where c^*_{NP} is the overlap concentration of the SCNPs). It has to be noticed that a fraction of the functional groups remains unreacted after the induced crosslinking during synthesis. A second option was using linear deuterated PMMA chains of different molecular weights as crowders. These molecules are chemically inert as opposed to SCNPs which can still react upon contact in suspension. This study confirmed coarse-grained MD-results on the analogous systems, showing a tendency of collapse of the SCNPs when the overall concentration of the solution exceeded the c^*_{NP}-value. The collapsing effect, manifested by the

decrease of both the chain dimension and the compaction revealed by the scaling exponent ν, becomes more pronounced with increasing concentration. The bulk limit was reported on a nanocomposite where PMMA-based SCNPs were dispersed on a polyethyleneoxide matrix [8], confirming the simulation results indicating crumpled globular structure.

Though these contributions represent a significant step forward in the field, a fundamental question is to check whether the universality of the results obtained by MD-simulations can be translated to real systems with SCNPs of different chemical nature, morphologies and kind of intrachain bonds. At high concentrations, following the predictions of the MD-simulations, compression by crowders is expected. However, as in solutions of PMMA-based SCNPs, aggregation of the real nano-objects can happen under certain conditions. The degree of internal compaction in such a case could change with respect to that in the unimers in good-solvent conditions. On the other hand, given the softness and penetrability of nano-particles and crowders, effects like swelling and interpenetration could also be present, leading to an increase of the volume occupied by the macromolecule and of the scaling exponent. Last, considering also the (soft) colloidal nature of SCNPs solutions, questions of universal scope like the effect of chemical nature and size of the crowders on the stabilization of the particles arise. If small enough, crowders could induce depletion destabilizing the suspension. Thus, crowded suspensions containing SCNPs can present an intriguing and rich phenomenology worth to be carefully scrutinized by microscopic techniques.

In this work we contribute to this field by investigating the structural properties of irreversible SCNPs based on polystyrene (PS) in a good solvent, where inert linear crowding PS macromolecules are present at different concentrations. The SCNP-signal could be differentiated from the crowders by small-angle neutron scattering (SANS) via index-matching deuterated crowders to the solvent. The effects of two linear crowding molecules of low and high molecular weight have been explored, and compared with the behavior of dilute SCNPs

suspensions. Molecular weight polydispersity effects have been carefully taken into account, allowing discriminating aggregates. Our model allows an estimation of the average mass of these aggregates, as well as simultaneously the size of the individual SCNP building units within them. The analysis of the results shows that the two kinds of crowders induce a very different effect on the SCNPs: while the long linear chains stabilize the suspension impeding the aggregation of SCNPs above the overlap concentration of the crowders c*, the short ones are found to mediate depletion.

Materials and methods

Synthesis of SCNPs. SCNPs were prepared from a random copolymer containing styrene (S) and azidomethyl styrene (AMS, 30 mol%) repeat units following the synthesis procedure described by Gonzalez-Burgos et al [38]. First, copolymerization of styrene (S) (2 ml, 17.4 mmol) and p-chlorostyrene (CMS) (0.6 ml, 4.3 mmol) was carried out using 4,4´-azobis(4-cyanovaleric acid) (1.7 mg, 6.1 x 10^{-3} mmol) as initiator. The reaction mixture was degassed by passing argon for 15 min and then stirred for 3 h at 80 ºC. After that, the resulting poly(S-co-CMS) copolymer was redissolved in a minimal amount of tetrahydrofuran and added to a large excess of methanol. The copolymer was isolated by filtration and further dried at room temperature (RT) under dynamic vacuum. Next, poly(S-co-CMS) (350 mg, 0.91 mmol CMS) was dissolved in N,N´-dimethyl formamide (DMF) (14 ml) at RT. Then, NaN_3 (2 eq., 116.5 mg) was added and the mixture was maintained under stirring for 24 h. After reaction completion, the system was concentrated and precipitated in a mixture of methanol/water (1:1). The resulting poly(S-co-AMS) copolymer was dried in a vacuum oven at RT under dynamic vacuum. Finally, poly(S-co-AMS) (50 mg, 0.617 mmol) was dissolved in DMF (50 mL) at RT. Then, the mixture was heated to 200 ºC under microwave irradiation (300 W, 150 psi) and maintained there for 30 min. The system was then cooled down to RT and concentrated in a

vacuum line using Schlenk flasks. The resulting SCNPs were isolated by precipitation in a mixture of methanol/water (1:1) and dried in a vacuum oven at 40ºC under dynamic vacuum.

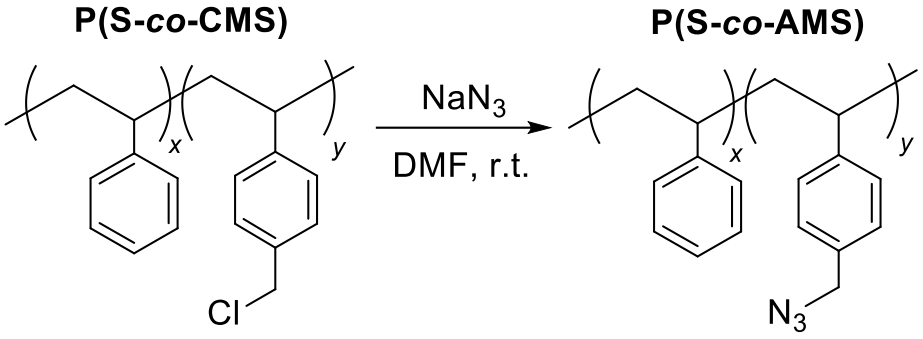

Scheme 1: Synthesis of poly(styrene-co-azidomethyl styrene) copolymer precursors. In the samples investigated in this work, x=0.70 and y=0.30.

Physico-chemical parameters of the SCNPs and their mass distribution obtained by GPC are summarized in Table 1. The neutron scattering length density of the solvent is 6.36 x10^{10} cm^{-2}, and its density 1.035 g/cm^3. Along this paper we consider as reference unit in our SCNPs or precursor what we call an 'effective' monomer, which properties result of averaging over the copolymer components. For example, the molar mass m_o of the effective monomer is obtained from those of the PS and AMS monomers as 0.70*$m_{o,styrene}$ + 0.30* $m_{o,AMS}$. Thus, the molar mass of an 'effective' monomer (from now on, we will call it just 'monomer') is 120.66 g/mol, which leads to N_{mono} = 1870 monomers in a SCNP molecule of number average molecular mass M_n=225.6kg/mol. The average radius of gyration R_g and scaling exponent ν of individually dispersed nanoparticles in dilute conditions have been determined by DLS and SAXS (see below). The value of R_g has been used to estimate the overlap concentration defined as c* = m/$(2R_g)^3$, where m is the mass of a single molecule. A fraction of unbonded reactive groups after synthesis of about 47% has been estimated from ^{1}H-NMR. These functional groups shall be responsible for intermolecular aggregation at high concentration.

	SCNP	dPS_A	dPS_B
M_w (kg/mol)	293.3	305	9.0
M_n (kg/mol)	225.6	282	8.8
PI	1.3	1.08	1.02
ρ (g/cm^3)	1.058	1.12	1.12
SLD (10^{10} cm^{-2})	1.71	6.41	6.41
ν	0.475	0.59	0.59
R_g (nm)	16	19.3	2.5
c* (mg/mL)	11	8	118

Table 1: Molecular parameters of SCNPS and two crowders (dPS_A and dPS_B): molecular masses and polydispersity index, density, scattering length density, exponent ν, average radius of gyration of individual molecules in dDMF and overlap concentration.

Sample formulation: Deuterated linear polystyrene crowding molecules of two different masses termed dPS_A and dPS_B have been used. Their dimensions have been determined by SAXS and DLS, respectively; molecular parameters and in particular c* are given in Table 1. dPS_A and SCNPs being of approximately same mass, their overlap concentrations are similar, around 10 mg/mL, whereas the much shorter dPS_B chains overlap only above $c^* \approx 120$ mg/mL. After synthesis and purification, stock solutions at c_{NP} = 2mg/mL of SCNP in dDMF (volume fraction Φ = 0.19%v) have been prepared, and appropriate quantities of dPSA or dPSB immediately added to reach the desired total concentration ranging from $c_{tot} = c_{NP} + c_{PS} =$ 5 to 100 mg/mL for dPS_A, and from c_{tot} = 80 to 400 mg/mL for dPS_B. Throughout this paper, c_{tot} is given to characterize sample concentrations. Although it might be suggested by the presentation of parameters as a function of total concentration, one should keep in mind that solutions were not made by continuous addition of polymer to an initially diluted solution. Instead, to different solutions containing diluted and non aggregated SCNPs, appropriate amounts of crowders

(deuterated polystyrene chains either dPS_A or dPS_B) were added to obtain the target value of the total concentration. Samples denoted SCNP+dPS_A with c_{tot} = 5, 10, 20, 40 and 100 mg/ml were prepared from a solution containing SCNPs in deuterated DMF at 2 mg of SCNP/ml by adding 3, 8, 18, 38, and 98 mg of dPS_A per ml of solution, respectively. Samples denoted SCNP+dPS_B with c_{tot} = 80, 162, 225 and 400 mg/ml were prepared from a solution containing SCNPs in deuterated DMF at a concentration of 2 mg/ml by adding 78, 160, 223 and 398 mg of dPS_B per ml of solution, respectively. All samples were thus simultaneously prepared in parallel from the diluted and non aggregated SCNPs with immediate addition of the appropriate amount of polymer to obtain the target value of the total concentration. As we will show, depending on the mass and quantity, this may hinder (by steric interactions) or induce (via depletion) aggregation of the SCNPs.

SANS measurements: SANS experiments were performed on the instrument KWS-2 at the Forschungs-Neutronenquelle Heinz Maier-Leibnitz in Garching. With an incident wavelength λ=5.27Å and using three sample-detector distances: 1.15, 5.76 and 19.76 m, a scattering vector q-range between 0.003 and 0.35 $Å^{-1}$ was covered. The solutions were filled in 2 mm thick Hellma Quarz cells. The azimuthally averaged scattered intensities were obtained as function of the wave-vector q. The signal from the background (solution of crowders) was measured under the same conditions and subtracted from the measurements on the solutions with labelled macromolecules. Experiments were carried out at room temperature.

SANS analysis: Due to the particular contrast conditions (see Table 1) only the SCNPs contribute to the scattering, while the crowding polymers are contrast-matched by the solvent. The basis of our modeling is to describe the scattering of an individual SCNP of well-defined mass (and thus R_g) by the general coil form factor P(q, R_g) [39]:

$$P(q, R_g) = \left[\left(\frac{1}{\nu U^{\frac{1}{2\nu}}}\right)\gamma\left(\frac{1}{2\nu}, U\right) - \left(\frac{1}{\nu U^{\frac{1}{\nu}}}\right)\gamma\left(\frac{1}{\nu}, U\right)\right] \quad (1a)$$

with

$$U = (2\nu + 1) \cdot (2\nu + 2) \cdot \frac{(qR_g)^2}{6} \quad (1b)$$

$$\gamma(a, b) = \int_0^b t^{a-1} e^{-t} dt \quad (1c)$$

This form factor is normalized to one at low q, and it is determined by two parameters, the radius of gyration, and the scaling exponent ν. The latter parameter will be determined independently from the high-q behavior of the scattered intensity

$$I(q) \propto q^{-1/\nu} \qquad \text{(high q)} \quad (2)$$

and is therefore not explicitly listed as an argument of $P(q,R_g)$. The form factor in eqs.(1) is closely related to the classical Debye form factor of ideal chains, but has the advantage to include a description of possibly non ideal chains ($\nu \neq ½$). In dilute suspensions of such monodisperse SCNPs, the total differential cross section per unit sample volume, for simplicity termed intensity I(q) here, is given by the product of various prefactors and $P(q, R_g)$:

$$I(q) = \frac{N}{V} \Delta\rho^2 V^2 P(q, R_g) \quad (3)$$

where N/V denotes the number density of SCNPs, Δρ is the scattering contrast given by the difference in scattering length density, and V is the (dry) volume of the SCNP, *i.e.* the number of monomers multiplied by the volume of each monomer. In presence of polydispersity in mass of the SCNPs, as determined by GPC (PI = 1.3, see Table 1), N/V becomes N_i/V, and the starting point of our scattering analysis in terms of the sum of form factors given below is obtained.

Results and discussion

Theoretical description of scattering of polydisperse unimers. As a starting point of our analysis, we have described the mass distribution obtained by GPC by a log-normal mass distribution for the volume fraction of molecules of monomer number i, $\Phi_i(i_0,\sigma)$:

$$\Phi_i(i_0,\sigma) = \frac{N_i}{V}V_i = \frac{\Phi}{\sqrt{2\pi}\sigma i}\exp\left(-\frac{ln^2\frac{i}{i_0}}{2\sigma^2}\right) \quad (4)$$

N_i/V represents the number density of chains of number of monomers i, thus describing chain mass. The log-normal distribution contains two parameters, i_0 and σ. From the properties of the moments of log-normal distributions, the average number of monomers is given by $N_{mono} = i_0 \exp(\sigma^2/2)$, while the polydispersity is given by $PI = \exp(\sigma^2)$. It follows that $i_0 = 1641$ and $\sigma = 0.51$. The corresponding log-normal distribution function is termed 'original GPC' and is displayed in Figure 1.

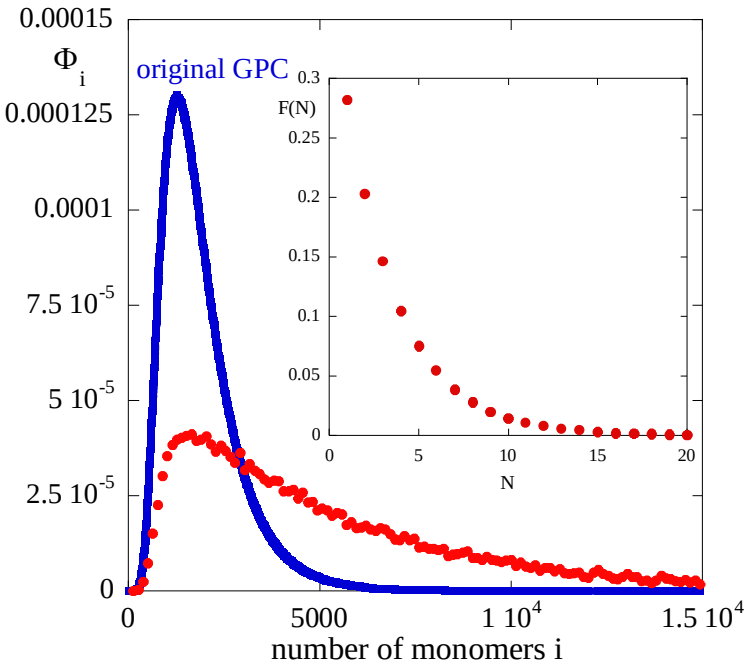

Figure 1: Φ_i mass distribution functions of SCNP as a function of the number of monomers, normalized to the total SCNP volume fraction by $\Sigma\Phi_i = V^{-1}\Sigma(N_iV_i) = \Phi$. The blue squares are given by the log-normal distribution function representing the mass distribution of SCNPs as obtained from GPC after synthesis according to eq. (4). The red circles correspond to a modified mass distribution function as explained in the text. Inset: the aggregation number distribution used to calculate the modified SCNP-mass distribution, with $N^* = 3$ and $\langle N \rangle = 3.5$.

The scattering of the individual SCNPs is described in the methods section. It needs to be completed by an expression for the radius of gyration $R_g^{(i)}$ of each SCNP containing i monomers. As the high-q power law of I(q) is found to be proportional to $q^{-1/\nu}$, this suggests a locally fractal structure of dimension 1/ν. The radii of gyration are then given by:

$$R_g^{(i)} = a\, i^{\nu} \tag{5}$$

where a is a general prefactor independent of i, specific for each molecule: a_{styr} for crowders, a_{prec} for precursor molecules, and a_{NP} for SCNPs. It should be noted that a becomes the fit parameter describing the relationship between molecular mass and spatial extent. Although there will be in general no visible Guinier plateau in the scattered intensities, this parameter will be fixed unambiguously as it is constrained by the GPC-results describing the mass and thus the low-q scattering limit, and the measured high-q power law. The determination of the radii of gyration of the single chains will thus be robust.

The total scattering of the polydisperse assembly of molecules defined by the mass distribution N_i/V is obtained by adding the contributions for each SCNP-mass (given by i) in absence of interactions. The total scattered intensity then reads:

$$I(q) = \sum_i \frac{N_i}{V} \Delta\rho^2 V_i^2 P\left(q, R_g^{(i)}\right) \tag{6}$$

Finally, the aggregation model developed below will be based on the description in terms of chain mass distribution introduced by eq. (4). It will lead to a modification of Φ(i) as exemplarily shown in Figure 1. To calculate the resulting intensity, the new distribution function replacing the one of eq.(4) is then injected in eq. (6). In practice, the new Φ(i) will be calculated from an aggregate distribution function having a single parameter N^* as defined below. An example of such an aggregate distribution function has been plotted in the inset of Figure 1. The specific distribution function shown here corresponds to ca. 28% of all aggregates

being SCNP-unimers, about 20% doublets, etc., and aggregates made of more than N = 15 SCNPs become exceedingly rare.

Characteristic sizes of isolated crowders and SCNPs in solution (DLS and SAXS). The size and conformation of the crowding polymer molecules at high dilution has been measured by DLS and SAXS in DMF solution for both masses, dPS_A and dPS_B. The resulting average radius of gyration varies with the number of monomers according to eq. (5), with a_{styr} = 1.9 Å and ν = 0.59, *i.e.* the expected exponent under good solvent conditions, which is in fact observed from the SAXS experiments. The radii of gyration and the corresponding overlap concentrations c* are given in Table 1. Considering that the Kuhn segment in PS consists of about 7 monomers [32], the radius of gyration of a Kuhn segment is thus ≈ 6Å, which we take as a measure of local stiffness. One may also note that the crowder molecules are highly monodisperse.

For the copolymer precursor of the SCNPs we have measured the hydrodynamic radius by DLS and obtained R_h=14.2 nm. Using $R_g = 1.77*R_h$ (ν = 0.59) [40], the radius of gyration of the precursors is 25.1 nm. It would correspond to a_{prec} = 3 Å in eq. (5). These precursor chains are stiffer than the pure PS, *e.g.* for 7 (recall: 'effective') monomers – which have the same number of main-chain atoms than 7 PS monomers –, $R_g \approx 9.5$ Å.

With SCNP suspensions, special care has been taken to avoid aggregation. Freshly synthesized SCNPs in dilute DMF solutions have been characterized using DLS, giving R_h = 10.6 nm at 1 mg/mL. Assuming $\nu \approx 0.5$: $R_g = 1.5*R_h$ [34], this value of R_h can be converted in the radius of gyration: $R_g \approx 16$ nm. SCNPs are thus smaller than their precursors, due to the internal bonds created during nanoparticle synthesis. SCNPs precipitated and stored after synthesis so that they could not react and form aggregates, were prepared at higher concentrations (2 and 5 mg/mL) in dDMF and investigated with SAXS. These experiments reveal the same results: R_g = 17.5

nm with ν = 0.48 at 2 mg/mL, and 13.3 nm with ν = 0.47 at 5 mg/mL. It results thus that freshly dissolved unimolecular SCNPs are correctly described by a radius of gyration of ca. 16 nm, and ν = 0.475, which are the values reported in Table 1 together with their c*. Thus, the value of the scaling exponent found (very close to ½) implies that the macromolecules follow a nearly Gaussian chain statistics. In this article, we refer to this size as the one of 'individually dispersed', or native SCNPs at high dilution, as opposed to the size of an individual SCNP being the building block of a higher order assembly. The R_g- and ν-values correspond to a_{NP} = 4.5 Å in eq. (5), with *i* representing again the number of effective monomers. The values of ν and a_{NP} translate in a higher local stiffness, presumably due to the existence of internal loops. For the reference 'segment' of 7 monomers, we thus have a dimension of $R_g \approx 11.5$ Å.

As mentioned above, aggregation effects shortly after sample preparation were investigated by Gonzalez-Burgos et al[37] for solutions of PMMA-based SCNPs. They showed propensity to aggregate for concentrations higher than about c*/3. Given the timing between sample preparation and SANS experiments reported below (time lapse of about ten days, including sample transportation), we have checked by DLS that there is no aggregation of our pure PS-based SCNPs in DMF at low concentration (1 mg/mL) over more than one month, whereas 2 mg/mL solutions show some aggregation after about 2 weeks (see Supporting Information). It is concluded that the sample series under scrutiny by SANS with 2 mg/mL of SCNPs and possibly those with added crowder molecules may start aggregation after sample formulation and before the SANS experiments. In the following, we describe the SANS results, which, as explained above, reveal the structure of the SCNPs in solutions with different degree of crowding.

Solution of only SCNPs (SANS): The structure of SCNPs at 2 mg/mL in dDMF has been measured by SANS and the intensity is plotted in Figure 2. It is compared to the intensity fitted using eq. (6), with the initial GPC-mass distribution function as shown in Figure 1 used as input.

The only fit parameters are thus ν obtained from the high-q slope as described in the methods, and a_{NP} defined by eq.(5) setting the size of the SCNPs.

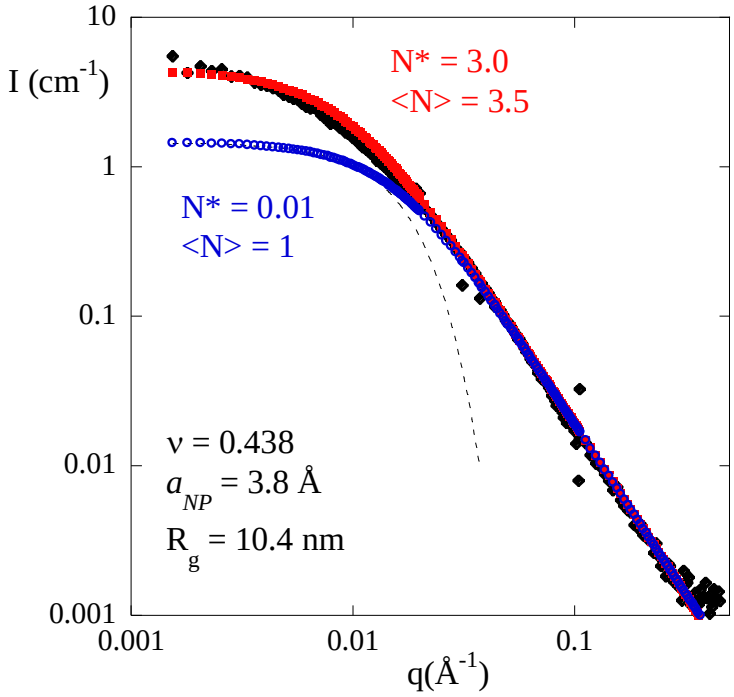

Figure 2: Scattered intensity I(q) as a function of wave vector q of SCNPs (c_{NP} = 2 mg/mL) in dDMF without added polymer (black diamonds) compared to the calculation (blue circles, no aggregation, <*N*> = 1) using eq. (6) with the mass distribution derived from the GPC measurement, with fit parameters as given in the legend. The average R_g of individual SCNP is determined by a Guinier fit (black dotted line). In red squares, the best fit using the aggregate model of polydisperse SCNPs as described in the text with *N** = 3 (<*N*> = 3.5).

The quality of the fit is very good in the power-law domain at high q, which is to be expected given the nature of the chain model given in the methods section. The value of ν of 0.438 corresponds to a chain which is more compact than ideal ones, of fractal dimension larger than two (1/ν = 2.3), which is also compatible with a denser molecule. This change in statistics as compared to the individually suspended SCNPs discussed above (ν = 0.475) is a first indication of conformational changes induced in the pure SCNP samples at 2 mg/mL studied by SANS.

A second indication is the value of a_{NP} which has decreased from 4.5 Å in individual suspension to 3.8 Å. The combination of both modifications results in a decrease of the SCNP size, first from the linear precursor to individual SCNPs due to internal crosslinking as shown by SAXS, and then further in the samples measured by SANS. We will see that this is caused by aggregation, which is visible in the low-q scattering, where the GPC calculation predicts a too low intensity. One may note that due to the large mass of the nanoparticles (for details see methods), c* is rather low (about 10 mg/mL), and the low concentration studied here (2 mg/mL) is only a factor of five below the overlap concentration. This implies that SCNPs imagined as spherical colloids have 'surface-to-surface' distances which are of the same order of magnitude as the radius of gyration (ca. 1.4 R_g), and one may easily imagine collisions within the solution and potential aggregation after some time.

In spite of aggregation, it is instructive to analyze the average radius of gyration corresponding to the GPC mass distribution of individual molecules combined with the experimentally measured, size determining – see eq. (5) – parameters a_{NP} and ν, by fitting a Guinier expression to the low-q intensity in Figure 2. The result corresponds to the typical size of individual SCNPs building blocks in the SANS suspension, *i.e.* as within aggregates. Their radius of gyration amounts to 10.4 nm. This is considerably smaller than the R_g of individually dispersed SCNPs (16 nm), and confirms what has been deduced from the evolution of a_{NP} and ν: in low concentration SANS samples, SCNPs are smaller than individually dispersed molecules, and their compaction might be due to aggregation.

The GPC-fit function in Figure 2 thus corresponds to SCNPs highlighted within their environment. The actually measured intensity deviates strongly from the GPC-fit at small q-values, by approximately a factor of three in the overall intensity. The prefactors of I(q) in eq.(6) are defined by the chemistry: the molecular volumes given by chromatography, as well as contrast and total concentration. The experimental low-q intensity exceeding the GPC-

prediction implies that the masses (or volumes) are larger than the ones of individual SCNPs, and that they are correlated on the scale of observation 1/q. This implies that chains form higher order assemblies, or aggregates: the low-q increase is caused by aggregation of SCNPs in suspension. From a simple analysis of the low-q limits of the fit and the experimental intensity plotted in Figure 2, one can estimate the average aggregation number to about three for pure SCNPs, supposing monodispersity. The exact average aggregation number can only be known if polydispersity is included in the calculation, which is the second ingredient of our aggregation model to be introduced now.

Model for aggregation of polydisperse SCNPs. There are different ways to incorporate aggregation in the model of the scattered intensity given by eq. (6). For monodisperse nanoparticles of known interaction, e. g. sticky hard-sphere like [41], one could calculate the structure factor contribution. Unfortunately, interactions here are unknown, possibly include SCNP interpenetration, and this does not seem feasible here. Moreover, one would have to define size-dependent interactions in order to describe polydisperse assemblies, and sum up the partial structure factors. We have therefore opted for a simpler model which appears to be appropriate for the present macromolecular systems of low density.

In Scheme 2, the concept of the model is illustrated: the assembly of two SCNPs is thought to lead to a hypothetical new single SCNP of mass equal to the sum of the masses of the parent SCNPs. The main assumption of our model is that the chain statistics of the aggregate is unperturbed with respect to the individual SCNPs, and described by eq. (5), with the same parameter a_{NP} as the individual nanoparticles.

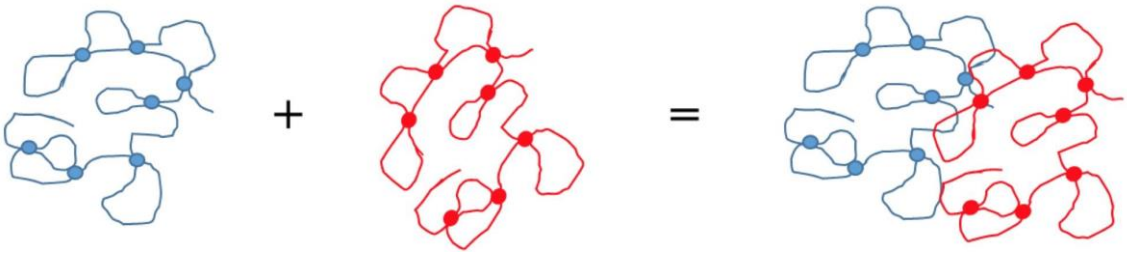

Scheme 2: Schematic representation of the aggregation process of two SCNPs of monomer numbers i_1 and i_2 described by the addition of their individual SCNP masses, and obeying the same local chain statistics.

The process shown in Scheme 2 describes the formation of a larger molecule out of two smaller parent molecules. Naturally, the generalization to arbitrary numbers of SCNPs aggregated in one assembly is straightforward: one simply has to add the masses, or corresponding numbers of monomers. One thus needs to calculate the sum $\Sigma\, i_k$ and inject the result into eq. (5) in order to obtain the new radius of gyration, while the local structure described by ν remains unchanged. A direct consequence of this aggregation process is that it modifies the distribution function of masses given by N_i/V, as now some smaller masses disappear while a new SCNP with larger mass given by the sum of its ingredients appears. The function is thus broadened and shifted towards higher *i*, as already illustrated in Figure 1 where the low-mass peak of the original GPC function is seen to decrease, and a high-mass tail is generated.

The last ingredient of the model is how to define the state of aggregation. We have opted for a very simple aggregate distribution function, giving the number fraction of aggregates made of single SCNPs, of doublets, triplets, etc… If we call *N* the aggregation number, *i.e.* the number of SCNP participating in a given aggregate, we can define the *discrete* distribution function of *N* as a single exponential decay:

$$F(N) = A\, e^{-N/N^*} \qquad (7)$$

where N^* is the only parameter of the distribution, and A is a normalization constant depending on N^*. Due to the discretization over doublets, triplets, and generally multiplets, the properties of the exponential function are somewhat counter-intuitive. For instance, a very small value of N^* ($N^* \ll 1$) corresponds to only single SCNPs, *i.e.* an average aggregation number $\langle N \rangle$ of one. Such a small N^* together with the experimentally determined a_{NP} and ν has been used to generate the GPC-model curve in Figure 2. It allowed us to highlight the individual SCNP size in an aggregated environment. For larger N^*, $\langle N \rangle$ grows with N^*. For simplicity, results will be given in terms of the average aggregation below.

In the proposed model for aggregation of polydisperse SCNPs, N^* is the only fit parameter for aggregation. It can be adjusted independently after having determined the best values of a_{NP} and ν from the intermediate- and high-q fit. In practice, it has been implemented via a Monte Carlo procedure repeatedly selecting randomly molecules of mass i from the initial mass distribution function, the number of molecules to be assembled being determined by eq. (7). The such obtained fitting curve for the intensity of the SCNPs in dDMF is shown in Figure 2, leading to $N^* = 3$, or equivalently $\langle N \rangle = 3.5$. The fit is found to be of acceptable quality given the simplicity of the process described in Scheme 2. The corresponding modification of the mass distribution is shown in Figure 1, with the aggregate distribution following eq. (7) displayed in the inset.

SCNP conformation in presence of long and short crowder molecules (SANS). Because of the contrast-matching of the dPS-crowders, the scattering measured in dPS-containing SCNP-suspensions is only due to the single-chain nanoparticles. In Figure 3a, the series of intensities for samples prepared with increasing amounts of the long chains, dPS_A, is plotted.

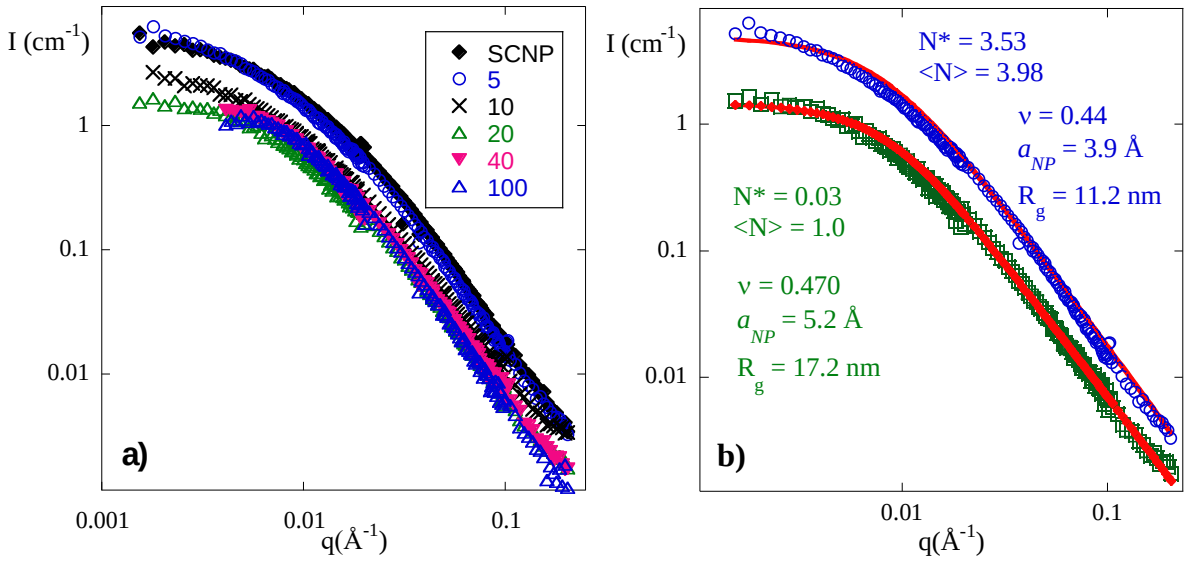

Figure 3: (a) Scattered intensities I(q) of SCNPs (c_{NP} = 2 mg/mL) in samples of increasing amount of long PS chains (dPS_A), the total concentration c_{tot} being given in the legend (mg/mL). **(b)** Examples of fits for c_{tot} = 5 (blue circles) and 20 mg/mL (green triangles), respectively, with fits (red diamonds), and parameters given in the legend.

The intensities are found to have a very similar shape: a Guinier-like plateau in the low-q range, followed by a crossover to a high-q scattering of roughly identical slope. However, there is a difference in the general intensity level, the two low-concentration samples (only SCNPs, and c_{tot} = 5 mg/mL) having a higher intensity than the rest of the series. This reflects lower aggregation numbers and higher radii of gyration of each SCNP for the samples with higher polymer content. Fits of only the high-q portion of the scattering data gave a first estimation for ν, shown in Table 2 and Figure 4a. Applying the aggregation model with these ν-values reveals that for c ≥ c*, the values of N^* are very small, i. e., no appreciable aggregation is found. We also note that for concentrations close to c*, the ν-value (as well as the R_g-value, not shown) is similar to that observed in the individual SCNPs (see Fig. 4a). Increasing the concentration, there is a tendency of the ν-value to diminish. Then, to decrease the scattering of the other fit parameters, we fixed the values of ν to the behavior indicated by the dashed lines in Figure 4a. It consists of a constant ν-value of ν = 0.44 below c* and a law

$$\nu = 0.52 - 0.04 \log(c_{tot}) \quad (8)$$

above c*. Two exemplary fits are shown in Figure 3b, for c_{tot} = 5 and 20 mg/mL, respectively, as well as in Figure 2 for the solution containing only SCNPs. The fit parameters are the SCNP conformation prefactor a_{NP} as defined by eq. (5) and the aggregation parameter N^* in eq. (7). Their values are reported in Table 2. Panels b and c in Figure 4 display the concentration dependence of the corresponding average radii of gyration determined by a Guinier fit, and aggregation numbers, respectively.

Solute	**c_{tot} (mg/mL)**	**ν**	**ν (smooth)**	**a_{NP} (Å)**	**N***	**<N>**	**R_g (nm)**
SCNP	2	0.438	0.440	3.6	3.00	3.50	10.4
SCNP+dPS$_A$	5	0.446	0.440	3.9	3.53	3.98	11.2
SCNP+dPS$_A$	10	0.475	0.483	4.2	1.16	2.02	16.3
SCNP+dPS$_A$	20	0.473	0.470	5.2	0.03	1.00	17.2
SCNP+dPS$_A$	40	0.456	0.458	5.3	0.49	1.27	15.6
SCNP+dPS$_A$	100	0.431	0.442	5.9	0.38	1.20	15.5
SCNP+dPS$_B$	80	0.465	0.446	3.8	2.50	3.43	10.8
SCNP+dPS$_B$	162	0.453	0.434	3.9	2.79	3.73	10.7
SCNP+dPS$_B$	225	0.417	0.428	4.5	1.77	2.70	11.2
SCNP+dPS$_B$	400	0.409	0.418	2.8	24.6	25.5	7.0

Table 2: SANS fit parameters. Sample type, total concentration, exponent ν from high-q fit, exponent ν smoothed and imposed in the application of the model, monomer parameter, aggregation parameter and average aggregation number, and average radius of gyration of SCNPs. The values of the four last parameters are obtained by fixing the given ν-values.

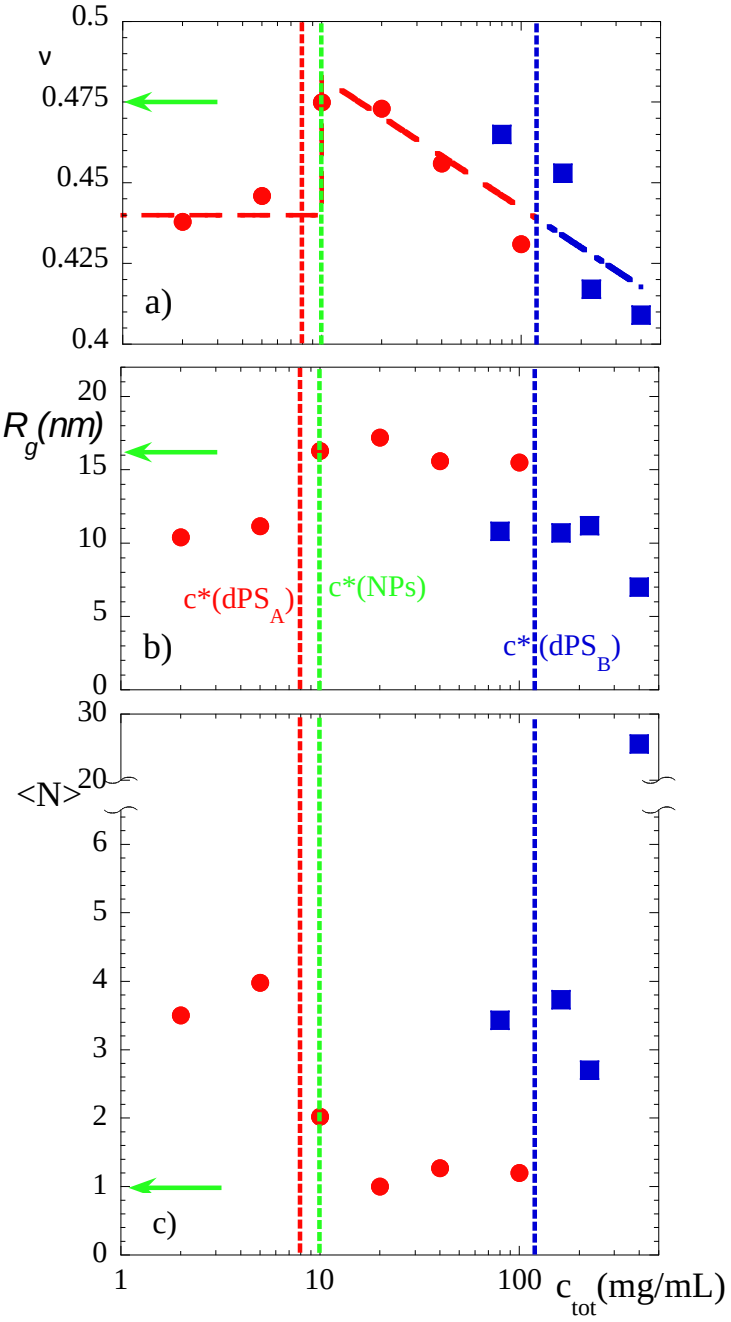

Figure 4: Evolution of the fit parameters with the total concentration c_{tot}. Red circles correspond to the long-chain system (dPS_A), blue squares to the short-chain system (dPS_B). The overlap concentrations c* of the three kinds of macromolecules are indicated by vertical lines and the values of the parameters corresponding to native individual SCNPs are indicated by the horizontal arrows. **(a)** High-q fit parameter ν. **(b)** Average radius of gyration R_g of individually highlighted SCNPs. **(c)** Average aggregation number <*N*>. The dashed lines in (**a**) show the behavior assumed for the ν-parameter to apply the model and determine the rest of the parameters.

A second series of crowded solutions has been measured at the same SCNP concentration of 2 mg/mL, with increasing amounts of the short linear polymer dPS_B. Due to the lower molecular mass of dPS_B, its overlap concentration is much higher, $c^* \approx 120$ mg/mL, and samples have been prepared from just below to well above this threshold value. The scattered intensities have been plotted in Figure 5a. They are found to have again a very similar shape, overlapping with the function of the solution containing only SCNPs. The low-q limits are found not to evolve for any but the sample at highest crowder concentration, indicating a similar state of aggregation for the first four samples. The sample with the highest concentration displays a strong increase in overall intensity, which signifies a much greater degree of aggregation. Moreover, the shift in the high-q power law towards higher intensities demonstrates that the radius of gyration of each SCNP within these aggregates decreases considerably. The exact extent of this evolution has been analyzed using the aggregate model developed in the previous section. Again, the first values of ν deduced from the high-q fit are given in Table 2 and shown as symbols in Fig. 4a. We observe that they scatter around the prediction of the law imposed to the scaling exponent for the solutions with high-molecular dPS_A crowders via eq. (8). Therefore, we have imposed the same behavior for the scaling exponent in these solutions and applied the aggregation model. To illustrate the quality of the fits, two of them are shown in Figure 5b, for $c_{tot} = 80$ and 400 mg/mL, respectively. It is clear from the fit of the 400 mg/mL sample that a large part of the aggregated structure has been captured by the model, while a remaining low-q upturn representative of giant structures is beyond our level of description. All indications thus coincide for this sample: it is highly aggregated, presumably approaching phase separation. The fit parameters and their evolution are reported in Table 2.

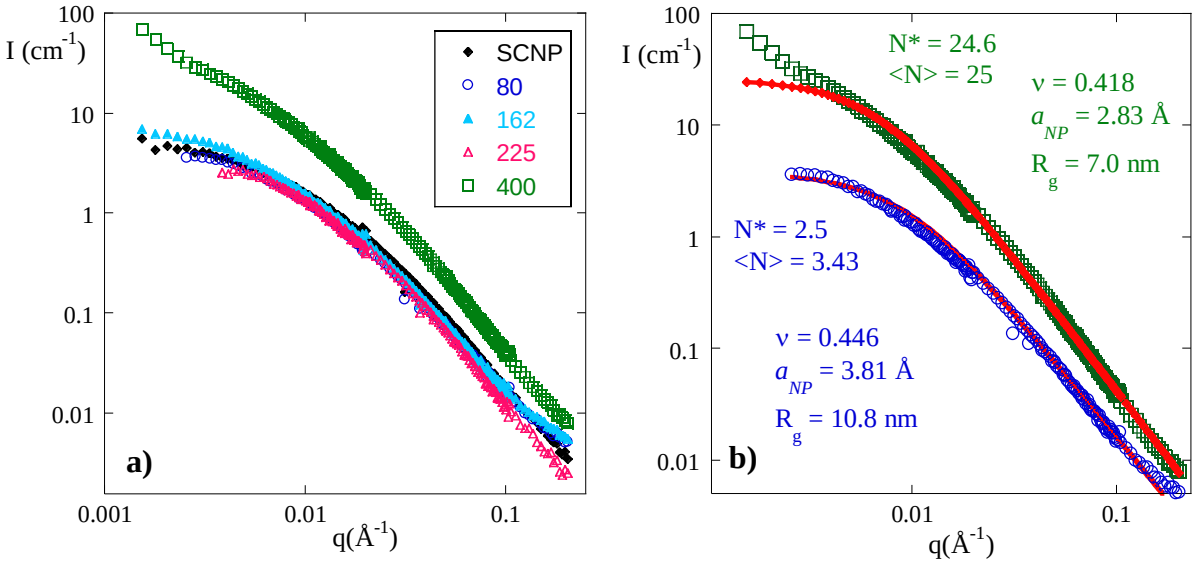

Figure 5: (a) Scattered intensities I(q) of SCNPs (c_{NP} = 2 mg/mL) in samples of increasing amount of short PS chains (dPS_B), the total concentration c_{tot} being given in the legend (mg/mL). **(b)** Examples of fits for c_{tot} = 80 (blue circles) and 400 mg/mL (green squares), respectively, with fits (red diamonds), and parameters given in the legend.

Phase diagram and comparison to simulations. A simple inspection of the SANS behavior at high and low-q values and the comparison with the expectation for a system of unimolecular SCNPs dispersion obeying the mass-polydispersity from GPC measurements points to the presence of aggregates and compression of SCNPs upon crowding. Beyond such semi-quantitative considerations, the proposed model, despite its simplicity, allows determining not only under which conditions the SCNPs form aggregates, but also their average number and deducing the conformation (average size and scaling exponent) of the macromolecules within them. It provides a very good description of the experimental results for the two kinds of crowding molecules.

We have observed that after about two weeks, SCNPs at a concentration of 2mg/mL aggregate. Even if this concentration is still a factor of five below their overlap concentration, the incessant collisions between the macromolecules in a molecular solvent facilitate their interactions,

leading apparently to the formation of new crosslinks – which now are of inter-molecular character – after some period of time. As it has been mentioned, these crosslinks are due to the presence of unreacted functional groups in the SCNPs after the synthesis procedure. This process also happens when a small fraction of big crowders are added to the solution. The aggregates formed consist of about four macromolecules in average. The macromolecules within these aggregates adopt a collapsed conformation with respect to that of the individual SCNPs as freshly produced: at low crowder concentrations, individual SCNP building blocks of aggregates have small radii of gyration, 10 to 11 nm, and scaling exponent of about 0.44, while the unimolecular SCNPs present a radius of gyration of about 16 nm and $\nu = 0.48$. We note that these aggregates seem to be stable, after monitoring them by DLS over more than two months (see SI).

Aggregation is however prevented –at least at the time scales between sample preparation and the SANS experiments—by adding high-molecular weight inert crowders at higher concentrations. In order to discuss the physics behind the evolution of the state of aggregation of the SCNPs crowded with the high-molecular weight linear chains, one has to compare the concentration to the overlap concentration c* of dPS_A given in Table 1. Apart from the sample with lowest concentrations (c_{tot} = 5mg/mL), the total concentration exceeds c*. The polymer chains overlap to form a sea of chains with embedded SCNPs. Under such conditions, no aggregation of SCNPs is evident (very small N^*); this is directly reflected by the jump in intensities in Figure 3, which coincides with the crossing of c*. The presence of big crowders has a two-fold effect in favoring the stabilization of the SCNPs in solution: on the one hand, they fill the space between the SCNPs and prevent their direct contact, and, on the other hand, they increase the viscosity of the medium and slow down dramatically the dynamics of the SCNPs, reducing enormously the frequency with which SCNPs directly interact with each other and can form new inter-molecular bonds. Therefore, after the same period of time after which

pure SCNPs in the solution form aggregates, in a solution of SCNPs prepared with high-molecular crowders close or above their overlap concentration their aggregation is arrested. Around c* (which is similar for both, SCNPs and long crowder molecules), SCNPs recover the radius of gyration they adopt in individually dispersed suspensions, ca. 16 nm and similar $\nu \approx 0.48$. With increasing concentration of crowders the SCNPs shrink as response to crowding. This effect is compatible with the decrease of the scaling exponent and the radius of gyration above c*. SCNPs keep their individuality and are compressed by neighboring crowders, by which they are completely surrounded. Such effect has been predicted from computer simulations, and has also been observed in solutions of PMMA-based SCNPs [37]. From the simulations, compaction symptoms (decrease in the values of the scaling exponent and the chain dimensions) are expected to be noticeable at the overlap concentration of the SCNPs. This prediction is also verified by our system.

With the shorter crowder, SCNPs aggregate at all concentrations investigated. The scenario in these solutions is dictated by the interplay between viscosity and depletion. Besides the atypical 400 mg/mL-case, the aggregates are composed by about four macromolecules –as in the case of the low concentrations below c^*_{NP}. Their radius of gyration within these aggregates is again around 10 nm. Thus, the conformation of the SCNPs within the aggregates seem to be quite similar independently of the crowding/viscosity/density of the surrounding medium of the aggregate ($c_{tot} < c^*_{NP} \approx 10$ mg/mL or $c_{tot} \approx c^*_{dPSb} \approx 100$ mg/mL). 'Self-crowding' effects seem to be the key ingredient in this kind of aggregates. For 400 mg/mL the size and scaling exponent decreases strongly and the number of macromolecules per aggregate grows to about 25. In such case, the aggregates are very large and bulk-like conditions are approached within them, with the expected crumpled globule conformation in the limit of absence of solvent, as predicted by the MD-simulations [8].

Conclusions

The conformational properties and aggregation of SCNPs suspended in a solvent and in presence of short and long crowder molecules have been studied by SANS. A specific structural model for aggregated SCNPs has been developed, based on the independently determined mass distribution of individual SCNPs together with a combination law treating an aggregate of molecules as one bigger one of identical total mass and scaling behavior. It is noted that polydispersity is thus a key ingredient of the model, because aggregate distribution functions are converted into mass distribution functions of hypothetical single chains. Moreover, we stress that the resulting conformational parameters, a_{NP} and ν, are uncoupled fit parameters which are obtained in a step-by-step procedure, starting from the high-q power-law to get ν first, followed by the determination of a_{NP} using the known low-q intensity of individually dispersed molecules (via known contrasts and masses from GPC), and finally N^* (or equivalently $\langle N \rangle$) allowing the description of the experimentally observed low-q increase caused by aggregation. An important result of our approach is that the radius of gyration of individual SCNPs embedded as building blocks in aggregates is determined, without having to employ complex chemistry and deuteration schemes like mixtures of H- and D-SCNPs under zero-average contrast conditions with simultaneous matching of crowders.

The main results of the impact of crowder molecules on SCNP suspensions may be summarized as follows: Native, freshly made SCNPs are not aggregated, and remain as individual macromolecules after long time periods of months if they are kept under the dilute conditions of the synthesis (≈1 mg/mL). At higher concentrations, even as low as about 5-fold below their overlap, pure SCNPs tend to aggregate moderately on time scales of days or weeks. This aggregation process is arrested by adding big inert crowder macromolecules above their overlap concentration. Their presence induces a huge increase of the viscosity of the surrounding medium, dramatically slowing down the kinetics of aggregation, and, more determining,

imposes steric barriers to the contacts between remaining reactive groups of different SCNPs. Upon crowding in such conditions, compression of the individual SCNPs is observed. With short crowder molecules, much higher concentrations need to be used to reach overlap. Due to depletion interactions caused by the entropic pressure exerted by the small molecules, moderate and finally catastrophic aggregation of SCNPs is induced. The SCNP conformational parameters demonstrate that native and aggregated SCNPs obey different chain statistics, the aggregated state progressively approaching the crumpled globular state. For similar moderate aggregation numbers (about four in average), SNCPs within aggregates are similarly compressed, independently of the surrounding environment ($c_{tot} < c^* \approx 10$mg/mL or $c_{tot} \approx c^*_{dPSB} \approx 100$mg/mL). Thus, the determining factor for chain statistics seems to the the 'self-crowding'. Huge aggregates obtained at extremely high concentrations provide bulk-like surroundings for the macromolecules, and there they seem to adopt very compact conformations approaching the proposed crumpled globular limit suggested by MD-simulations.

Thorough studies of SCNP structure in crowded environments are intended to contribute to the understanding of the behavior of intrinsically disordered nanoparticles and proteins in naturally dense, multicomponent media. Further studies, possibly based on computer simulations combined with experimental approaches, shall allow determining how exactly the conformation of disordered molecules is affected by the presence of linear or branched chains, investigate the degree of molecular interpenetration, and the way the osmotic pressure of the crowders is exerted on intrinsically disordered soft nano-objects.

Acknowledgements: Work presented here was initiated during a stay of JO in San Sebastian funded by DIPC (Donostia International Physics Center). Funding by DIPC, the European Network of Excellence Softcomp, the Basque Government (code: IT-1175-19) and the Ministerio de Economía y Competitividad (code: PGC2018-094548-B-I00 (MINECO/FEDER, UE)) is gratefully acknowledged. This work is based on experiments performed at KWS-2 (Heinz Maier-Leibnitz Zentrum (MLZ), Garching, Germany), and has been supported by the European Commission under the 7th Framework Programme through the 'Research Infrastructures' action of the 'Capacities' Programme, NMI3-II Grant Number 283883.

Supporting information: DLS results on PS-SCNPs at 1mg/mL and 2mg/mL.

References

(1) Mavila S.; Eivgi, O.; Berkovich, I.; Lemcoff, N.G.; Intramolecular Cross-Linking Methodologies for the Synthesis of Polymer Nanoparticles. *Chem. Rev.* **2016**, 116, 878-961.

(2) Altintas, O.; Barner-Kowollik, C. Single-Chain Folding of Synthetic Polymers: A Critical Update. *Macromol. Rapid Commun*. **2016**, 37, 29-46.

(3) Altintas, O.; Barner-Kowollik, C. Single Chain Folding of Synthetic Polymers by Covalent and Non-Covalent Interactions: Current Status and Future Perspectives. *Macromol. Rapid Commun.* **2012**, 33, 958-971.

(4) Sanchez-Sanchez, A.; Akbari, S.; Etxeberria, A.; Arbe A.; Gasser, U.; Moreno A. J.; Colmenero J.; Pomposo, J. A. "Michael" Nanocarriers Mimicking Transient-Binding Disordered Proteins. *ACS Macro Letters* **2013**, *2*, 491-495.

(5) Pomposo, J.A. Bioinspired single-chain polymer nanoparticles. *Polym. Int.* **2014**, 63, 589-592.

(6) Latorre-Sánchez, A.; Pomposo, J.A. Recent bioinspired applications of single-chain nanoparticles. *Polym. Int.* **2016**, 65, 855-860.

(7) Huo, M.; Wang, N.; Fang, T.; Sun, M; Wei, Y.; Yuan J. Single-chain polymer nanoparticles: Mimic the proteins. *Polymer* 2015, **66**, A11-A21.

(8) Moreno, A. J.; Lo Verso, F.; Arbe, A.; Pomposo, J. A.; Colmenero, J. Concentrated Solutions of Single-Chain Nanoparticles: A Simple Model for Intrinsically Disordered Proteins under Crowding Conditions. *J. Phys. Chem. Lett.* **2016**, *7*, 838-844.

(9) Arbe, A.; Pomposo, J. A.; Moreno, A. J.; Lo Verso, F.; Gonzalez-Burgos, M.; Asenjo-Sanz, I.; Iturrospe, A.; Radulescu, A.; Ivanova, O.; Colmenero, J. Structure and dynamics of single-chain nano-particles in solution. *Polymer* **2016**, *105*, 532-544.

(10) Moreno, A. J.; Lo Verso, F.; Sanchez-Sanchez, A.; Arbe, A.; Colmenero, J.; Pomposo, J. A. Advantages of Orthogonal Folding of Single Polymer Chains to Soft Nanoparticles. *Macromolecules* **2013**, *46*, 9748-9759.

(11) Müge, A.; Elisa, H.; Meijer, E.W., Anja, R.A.P. Dynamic Single Chain Polymeric Nanoparticles: From Structure to Function. In Sequence-Controlled Polymers: Synthesis, Self-Assembly, and Properties; American Chemical Society: **2014**; 1170, 313−325.

(12) González-Burgos, M.; Latorre-Sanchez, A.; Pomposo, J. A. Advances in single chain technology. *Chem. Soc. Rev.* **2015**, *44*, 6122-6142.

(13) Hanlon, A. M.; Lyon, C. K.; Berda, E. B. What Is Next in Single-Chain Nanoparticles? *Macromolecules* **2016**, *49*, 2-14.

(14) *Single-Chain Polymer Nanoparticles: Synthesis, Characterization, Simulations, and Applications*; Ed.: Pomposo, J. A.; Wiley-VCH: Weinheim, **2017**.

(15) Cheng, C.-C.; Lee, D.-J.; Liao, Z.-S.; Huang, J.-J. Stimuli-Responsive Single-Chain Polymeric Nanoparticles towards the Development of Efficient Drug Delivery Systems. *Polym. Chem.* **2016**, *7*, 6164−6169.

(16) Liu, Y.; Pujals, S.; Stals, P. J. M.; Paulöhrl, T.; Presolski, S. I.; Meijer, E. W.; Albertazzi, L.; Palmans, A. R. A. Catalytically Active Single-Chain Polymeric Nanoparticles: Exploring Their Functions in Complex Biological Media. *J. Am. Chem. Soc.* **2018**, *140*, 3423-3433.

(17) Kröger, A. P. P.; Paulusse, J. M. J. Single-Chain Polymer Nanoparticles in Controlled Drug Delivery and Targeted Imaging. *J. Controlled Release* **2018**, *286*, 326-347.

(18) Garmendia, S.; Dove, A. P.; Taton D.; O'Reilly, R. K. Reversible ionically-crosslinked single chain nanoparticles as bioinspired and recyclable nanoreactors for N-heterocyclic carbene organocatalysis. *Polym. Chem.* **2018**, *9*, 5286-5294.

(19) Guazzelli, E.; Martinelli, E.; Galli, G.; Cupellini, L.; Jurinovich, S.; Mennucci, B. Single-chain self-folding in an amphiphilic copolymer: An integrated experimental and computational study. *Polymer* **2019**, *161*, 33-40.

(20) Bajj, D. N. F.; Tran, M. V.; Tsai, H.-Y.; Kim, H.; Paisley, N. R.; Algar, W. R.; Hudson, Z. M. Fluorescent Heterotelechelic Single-Chain Polymer Nanoparticles: Synthesis, Spectroscopy, and Cellular Imaging. *ACS Appl. Nano Mater.* **2019**, *2*, 898-909.

(21) Romashchenko, A.V.; Kan, T.W.; Petrovski, D.V.; Gerlinskaya, L.A.; Moshkin, M.P. ; Moshkin, Y.M. Nanoparticles Associate with Intrinsically Disordered RNA-Binding Proteins; *ACS Nano* **2017**, 11(2), 1328-1339

(22) Habchi, J.; Tompa, P.; Longhi, S.; Uversky, V. N. Introducing Protein Intrinsic Disorder. *Chem. Rev.* **2014**, *114*, 6561-6588.

(23) Stadler, A. M.; Stingaciu, L.; Radulescu, A.; Holderer, O.; Monkenbusch, M.; Biehl, R.; Richter, D. Internal Nanosecond Dynamics in the Intrinsically Disordered Myelin Basic Protein. *J. Am. Chem. Soc.* **2014**, *136*, 6987-6994.

(24) Ramer, G.; Ruggeri, FS ; Levin, A; Knowles, TPJ ; Centrone, A; Determination of Polypeptide Conformation with Nanoscale Resolution in Water; *ACS Nano* **2018** 12(7), 6612-6619

(25) Banks, A.; Qin, S.; Weiss, K. L.; Stanley, C. B.; Zhou, H. X. Intrinsically Disordered Protein Exhibits Both Compaction and Expansion under Macromolecular Crowding. *Biophys. J.* **2018**, *114*, 1067-1079

(26) Candotti, M.; Orozco, M. The Differential Response of Proteins to Macromolecular Crowding. *PLoS Comput. Biol.* **2016**, *12*, e1005040.

(27) Liu, W.; Liu, X.; Zhu, G.H.; Lu, L.Y.; Yang D.W. A Method for Determining Structure Ensemble of Large Disordered Protein: Application to a Mechanosensing Protein; *J. Am. Chem. Soc.* **2018**, 140(36), 11276-11285

(28) Aiertza, M. ; Odriozola, I. ; Cabañero, G. ; Grande, H.J.; Loinaz, I. Single-chain polymer nanoparticles. *Cell. Mol. Life Sci.* **2012**, 69, 337-346.

(29) Liu, Y.; Pujals, S.; Stals, P. J. M.; Paulöhrl, T.; Presolski, S. I.; Meijer, E. W.; Albertazzi, L.; Palmans, A. R. A. Catalytically Active Single-Chain Polymeric Nanoparticles: Exploring Their Functions in Complex Biological Media. *J. Am. Chem. Soc.* **2018**, *140*, 3423-3433.

(30) Grosberg, A. Y.; Nechaev, S. K.; Shakhnovich, E. I. The role of topological constraints in the kinetics of collapse of macromolecules. J. Phys. 1988, 49, 2095-2100.

(31) L.A. Mirny, The fractal globule as a model of chromatin architecture in the cell. *Chromosome Res.* **2011**, *19*, 37-51.

(32) Rubinstein, M.; Colby, R. H. *Polymer Physics*; Oxford University Press, Inc.; New York, **2003**.

(33) Pravaz, O. ; Droz, B. ; Schurtenberger, P. ; Dietsch, H. The influences of the transfer method and particle surface chemistry on the dispersion of nanoparticles in nanocomposites, *Nanoscale*, **2012**, 4, 6856

(34) Houston, J. E.; Chevrier, M.; Appavou, M.-S.; King, S.M.; Clément, S.; Evans, R. C. A self-assembly toolbox for thiophene-based conjugated polyelectrolytes: surfactants, solvent and copolymerization. *Nanoscale*, **2017**, 9, 17481

(35) Koll, R.; Fruhner, L.S.; Heller, H.; Allgaier, J.; Pyckhout-Hintzen, W.; Kruteva, M.; Feoktystov, A.; Biehl, R.; Förster, S.; Weller, H. Creating a synthetic platform for the encapsulation of nanocrystals with covalently bound polymer shells. *Nanoscale*, **2019**, 11, 3847

(36) Le Coeur, C.; Teixeira, J.; Busch, P. ; Longeville, S. Compression of random coils due to macromolecular crowding: Scaling effects. *Phys Rev E* **2010**, 81(6), 061914

(37) González-Burgos, M.; Arbe, A.; Moreno, A. J.; Pomposo, J. A.; Radulescu, A.; Colmenero, J. Crowding the Environment of Single-Chain Nanoparticles: A Combined Study by SANS and Simulations. *Macromolecules* **2018**, *51*, 1573-1585.

(38) González-Burgos, M.; Alegría, A.; Arbe, A.; Colmenero, J.; Pomposo, J. A. An unexpected route to aldehyde-decorated single-chain nanoparticles from azides. *Polym. Chem.* **2016**, *7*, 6570-6574.

(39) Hammouda, B. Small-Angle Scattering from Branched Polymers. *Macromol. Theory Simul.* **2012**, 21, 372-381.

(40) De-La-Cuesta, J.; Gonzalez, E.; Moreno, A. J.; Arbe, A.; Colmenero, J.; Pomposo, J. A. Size of Elastic Single-Chain Nanoparticles in Solution and on Surfaces. *Macromolecules* **2017**, *50*, 6323-6331.

(41) Baxter, R.J. Percus-Yevick Equation for Hard Spheres with Surface Adhesion. *J. Chem. Phys.* **1968**, 49, 2770.

Table of contents graphics: